THE JOURNAL OF PHYSICAL CHEMISTRY A

pubs.acs.org/JPCA Article

Atom Assisted Photochemistry in Optical Cavities

Eric Davidsson* and Markus Kowalewski*

Cite This: J. Phys. Chem. A 2020, 124, 4672−4677

Read Online

ACCESS | Metrics & More | Article Recommendations | Supporting Information

ABSTRACT: Strong light−matter coupling can modify the photochemistry of molecular systems. The collective dynamics of an ensemble of molecules coupled to the light field plays a crucial role in experimental observations. However, the theory of polaritonic chemistry is primarily understood in terms of single molecules, since even in small molecular ensembles the collective dynamics becomes difficult to disentangle. Understanding of the underlying ensemble mechanisms is key to a conceptual understanding and interpretation of experiments. We present a model system that simplifies the problem by mixing two-level Mg atoms with a single MgH^+ molecule and investigate its collective dynamics. Our focus is on the modified chemical properties of a single diatomic molecule in the presence of an ensemble of resonant atoms as well as the structure of the major and intermediate polariton states. We present quantum dynamics simulations of the coupled vibronic−photonic system for a variable size of the atomic ensemble. Special attention is given to dissociative the dynamics of the MgH^+ molecule.

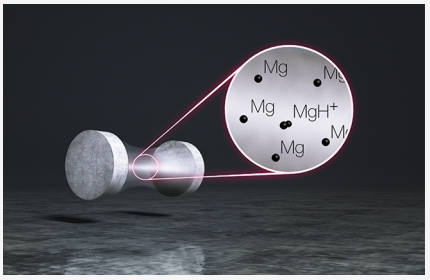

INTRODUCTION

Strong coupling of molecules with quantized photon fields in optical cavities can be observed when the Rabi frequency exceeds the spontaneous decay rate. A wide range of different experiments makes use of strong coupling in nanocavities.[1] A few examples of strong coupling with molecules include[2,3] spectroscopy on the polariton states,[4] modifications of intersystem crossing,[5] strong coupling in J-aggregates,[6,7] coherent control with quantum light,[8] vibrational strong coupling,[9,10] and strong coupling in plasmonic nanoparticles.[11] Strong coupling in nanocavities has been demonstrated to modify the reactivity of photochemical processes and to induce collective Rabi splittings on the order of hundreds of meV.[12−14] Here, the confined light field forms a hybrid state with molecular degrees of freedom. These hybrid states are also known as dressed states or polariton states and are best described by means of a quantized light field.[15] The molecular Jaynes−Cummings (JC) model has shown that strong light−matter coupling results in nonadiabatic dynamics,[16−18] analogous to avoided crossings and conical intersections.[19−22]

However, typical experimental parameters indicate that single-molecule strong coupling is rather an exception,[23] and prominent experiments instead rely on collective strong coupling[12−14,24] to modify the photochemistry. Consequently, the model has to be replaced by a molecular Tavis−Cummings (TC) model[17,22,25] to describe the dynamics correctly. All particles in the ensemble now act as one large collective quantum system. In the case of an atomic ensemble,[26] two polariton states will contribute to the dynamics, while $N - 2$ dark states remain virtually unpopulated. Even though corresponding states in the molecular TC model are often termed dark states, too, it has been demonstrated that these states fully contribute to the dynamics when nuclear degrees of freedom are introduced.[3,27] The resulting dynamics thus becomes more complicated as a large number of intermediate polariton states (previously decoupled dark states) are involved. Moreover, a similarly large number of collective vibrational degrees of freedom have to be included, making it increasingly difficult to disentangle the details of the reaction mechanism.

In this paper, we investigate a mixed molecular−atomic TC model.[28] This approach provides a simplified view of collective dynamics while keeping some features of the nuclear degrees of freedom at a reasonable computational cost. This allows us to gain more insight into the underlying mechanisms of collective couplings and its dynamics. The aim is to bridge the gap between a single molecule model and collectively coupled ensemble of molecules and to clarify the basic mechanisms of collective strong coupling and to investigate the question if the addition of atoms can be traded in for single-molecule coupling strength.

MODEL

Our model is comprised of a single MgH^+ molecule located in an antinode of a lossless cavity mode along with an ensemble of $N \in \{0, ..., 30\}$ Mg atoms. The MgH^+ and Mg particles are resonantly coupled to the quantized light field of the cavity

Received: April 30, 2020
Revised: May 11, 2020
Published: May 11, 2020

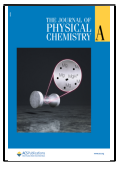

mode. Direct interactions between the particles are neglected. The first four electronic states of the MgH^+ molecule are considered and modeled under the molecular Born–Oppenheimer approximation as potential energy surfaces depending on the internuclear distance, q. The Mg atom is treated as a two-level system where the ground state and first electronically excited states are considered. Translational and rotational degrees of freedom are neglected in this model. The coupling between the cavity and matter degrees of freedom assumes the cavity Born–Oppenheimer approximation.[29]

The Hamiltonian of the system is constructed from the respective quantum systems and their interactions:

$$\hat{H} = \hat{H}_m + \hat{H}_a + \hat{H}_c + \hat{H}_{ca} + \hat{H}_{cm} \tag{1}$$

where $\hat{H}_m$, $\hat{H}_a$, and $\hat{H}_c$ describe the molecular, atomic, and photonic subsystems, respectively. $\hat{H}_{ca}$ and $\hat{H}_{cm}$ are the interaction terms between the cavity mode and either atoms or molecule, respectively.

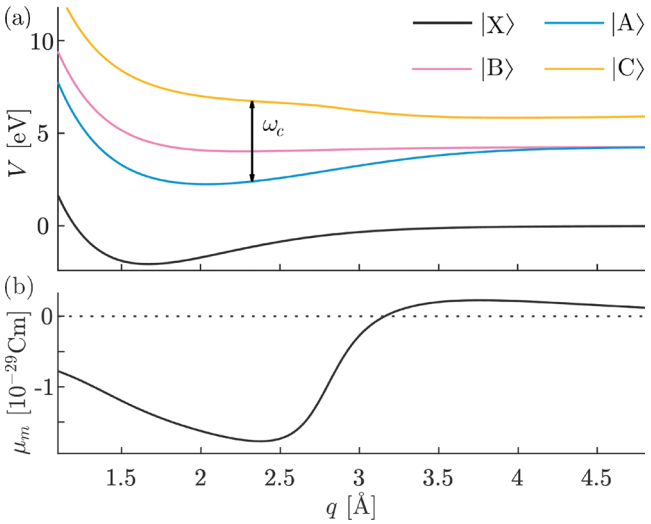

Figure 1. (a) Potential energy curves for the first four electronic states of MgH^+, calculated in ref 32. The cavity mode, ω_c, is tuned to be resonant with the $3s^2$ to $3s^13p^1$ transition of Mg, which implies resonance with the molecular transition between $|A\rangle$ and $|C\rangle$ at q = 2.23 Å. (b) Transition dipole moment between states $|A\rangle$ and $|C\rangle$ in the MgH^+ molecule.

The Hamiltonian for the molecular subsystem has two active electronic states $|A\rangle$ and $|C\rangle$, with their respective potential energy surfaces $V_A(q)$ and $V_C(q)$, as shown in Figure 1a, where q is the internuclear distance.

$$\hat{H}_m = -\frac{\hbar^2}{2m}\frac{d^2}{dq^2} + V_A(q)\hat{\sigma}_m\hat{\sigma}_m^\dagger + V_C(q)\hat{\sigma}_m^\dagger\hat{\sigma}_m \tag{2}$$

Here, $\hat{\sigma}_m = |A\rangle\langle C|$ and $\hat{\sigma}_m^\dagger = |C\rangle\langle A|$ de-excite and excite the molecule, respectively. For the atomic subsystem, the Hamiltonian is a sum of the N two-level systems.

$$\hat{H}_a = \hbar\sum_{n=1}^{N}\omega_a\,\hat{\sigma}_{a,n}^\dagger\,\hat{\sigma}_{a,n} \tag{3}$$

The atomic transition frequency, ω_a, is identical for all atoms. $\hat{\sigma}_{a,n} = |g_n\rangle\langle e_n|$ and $\hat{\sigma}_{a,n}^\dagger = |e_n\rangle\langle g_n|$ de-excite and excite the nth atom, respectively. The cavity mode has a frequency ω_c and interacts resonantly with both the MgH^+ molecule and Mg atoms.

$$\hat{H}_c = \hbar\omega_c\left(\hat{a}^\dagger\hat{a} + \frac{1}{2}\right) \tag{4}$$

The frequency ω_c is tuned such that $\omega_c = \omega_a$. This puts the resonance in the MgH^+ molecule to a bond length where the transition dipole moment has a maximum (compare Figures 1a and 1b). Here, $\hat{a}^\dagger$ and $\hat{a}$ are the photonic creation and annihilation operators, respectively. The interaction between cavity and molecule is given as

$$\hat{H}_{c-m} = \mathcal{E}_c\,\hat{\mu}_m(q)(\hat{a}^\dagger\hat{\sigma}_m + \hat{a}\hat{\sigma}_m^\dagger) \tag{5}$$

where we have assumed the rotating wave approximation and $\mathcal{E}_c = |\mathbf{E}_c|$ is the cavity vacuum electric field strength for a single photon in the ω_c mode. The polarization vector of the cavity, $\mathbf{E}_c$, is assumed to be aligned with the transition dipole vector, $\boldsymbol{\mu}_m$; thus, $\mathbf{E}_c\cdot\hat{\boldsymbol{\mu}}_m(q) = \mathcal{E}_c\,\hat{\mu}_m(q)$. The transition dipole moment $\mu_m(q)$ between states $|A\rangle$ and $|C\rangle$ is shown in Figure 1b. The electric field strength, $\mathcal{E}_c$, depends on the quantization volume of the cavity mode V:

$$\mathcal{E}_c = \sqrt{\frac{\hbar\omega_c}{2\epsilon_0 V}} \tag{6}$$

The interaction between cavity and atoms is given by

$$\hat{H}_{ca} = \sum_{n=1}^{N}\mathcal{E}_c\,\mu_a(\hat{a}^\dagger\hat{\sigma}_{a,n} + \hat{a}\hat{\sigma}_{a,n}^\dagger) \tag{7}$$

where we have also assumed the rotating wave approximation. The atomic transition dipole moment, $\mu_a = 1.981\times10^{-29}$ C m, sets the magnitude of the electromagnetic coupling between $|g_n\rangle$ and $|e_n\rangle$.

Equation 1 can be viewed as a generalized TC Hamiltonian comprised of an atomic[25] and a molecular TC[3,30] Hamiltonian. With $N > 0$ atoms, the diagonalization of eq 1 in the electronic subspace (i.e., without the kinetic energy from eq 2) results in $N - 1$ dark states that are uncoupled from three polariton states. Note that in the diagonal polariton basis the Born–Oppenheimer approximation no longer holds,[30,31] resulting in nonadiabatic couplings. Because we have employed the rotating-wave approximation in eqs 5 and 7, the model is generally valid for single-particle cavity couplings on the order of magnitude such that $\mathcal{E}_c\,\mu_{(a,m)} \ll \omega_m, \omega_a, \omega_c$ (with the typical ensemble size considered in this paper collective couplings remain on the same order of magnitude as single particle couplings). For the molecular Hamiltonian eq 2 we have assumed no couplings between nuclear and electronic degrees of freedom other than through the cavity light field. For simplicity, we have assumed lossless mirrors, which allows us to use the time-dependent Schrödinger equation rather than a Lindblad equation. This assumption requires that the photochemical process take place on a time scale shorter than the photon lifetime, which is also the requirement for strong coupling (see further discussions in the Supporting Information).

METHODS

The dynamics of the system are obtained by numerically solving the time-dependent Schrödinger equation with the Hamiltonian from eq 1. The wave function is propagated in the

https://dx.doi.org/10.1021/acs.jpca.0c03867
J. Phys. Chem. A 2020, 124, 4672–4677

product basis of molecular, atomic, and Fock states, which is called the product basis in the following. For analysis of the unitary time evolution, the wave function is transformed into a polariton basis, where eq 1 is diagonal in the subspace of electronic states and Fock states. This basis is called the polariton basis in the following. In this basis, the states experience nonadiabatic couplings in the form of derivative couplings at the points of resonance.[16]

Because of the rotating wave approximation in eqs 5 and 7, subspaces with different excitation numbers are decoupled, and the state space in the product basis can be truncated. By use of the excitation number operator

$$\hat{M} = \hat{a}^{\dagger}\hat{a} + \hat{\sigma}_m^{\dagger}\hat{\sigma}_m + \sum_{n=1}^{N} \hat{\sigma}_{a,n}^{\dagger}\hat{\sigma}_{a,n} \tag{8}$$

basis states can be excluded based on their excitation number. For example, with one molecule and two atoms in the cavity, we include basis states such as $|C, g_1, g_2, 0\rangle$, $|A, e_1, g_2, 0\rangle$, and $|A, g_1, g_2, 1\rangle$, for which $\langle\hat{M}\rangle = 1$. But states such as $|C, e_1, g_2, 0\rangle$ or $|A, g_1, e_2, 1\rangle$ for which $\langle\hat{M}\rangle > 1$ are excluded. This reduces the size of the Hamiltonian considerably and enables the treatment of larger ensembles of N atoms.

The potential energy curves (Figure 1a) and transition dipole moments (Figure 1b) for the MgH^+ molecule[32,33] are calculated with the program package Molpro[34] at the CASSCF(12/10)/MRCI/ROOS level of theory.[35,36] For the Mg atoms, we use the transition from the $3s^2$ ground state to the $3s^13p^1$ excited state, labeled as $|g_n\rangle$ and $|e_n\rangle$, respectively. The transition frequency ω_a is collected from Nist Atomic Spectra Database,[37] and the corresponding transition dipole moment is calculated with Molpro at the CASSCF(8/7)/MRCI/ROOS level of theory (following ref 32). The photon energy for the cavity, ω_c, is tuned to be resonant with the transition in the Mg atom, resulting in a wavelength of 285 nm.

The vibrational wave function and the potential energy curves are represented on a discretized grid in position space. The nuclear coordinate q is represented by 512 grid points in the interval between 1.10 and 8.05 Å. Reflections at the edge of the grid are suppressed by the absorption of wave packets with a perfectly matched layer[38] at the dissociation limit of each potential. Time evolution over 503 fs, with time steps of 24.2 as, is done with our in-house code (QDng) by using the Chebyshev propagation method.[39] The initial state, $|\Psi_0\rangle = \hat{\sigma}_{XC}^{\dagger}\hat{\mu}_{XC}|X, \nu_0\rangle$, is generated perturbatively by applying the transition dipole operator to the vibronic ground state of MgH^+ and is renormalized before propagation. Without a loss of generality, this method assures a consistent initial condition. This is in contrast with a classical pump pulse, for which the magnitude of the initial population changes rapidly as the electronic energies are shifted around by varying system parameters. We verified the approach with a second calculation where the system is pumped with a classical laser field $E(t)$ from $|X\rangle$ to $|C\rangle$ (see the Supporting Information).

The polariton diagonalization, which is used for analyzing the results, is performed independently for each discrete grid point along q. The eigenvalues are then associated between neighboring grid points by an algorithm that tracks their corresponding eigenvectors, with the following strategy. Each eigenstate $|\phi_i^{k+1}\rangle$, at grid point q_{k+1}, is associated with an eigenstate at the previous grid point, q_k, such that the overlap $|\langle\phi_i^k|\phi_j^{k+1}\rangle|^2$ is maximized. This is necessary to obtain a correct identification of the states from numerical diagonalization routines that order eigenstates by energy. In the case where the potential energy curves of uncoupled polaritonic states crosses (see Figures 3 and 4), energy ordering would lead to an artificial reordering of states between points on either side of the curve crossing. When tracking eigenvectors from the particular Hamiltonian in eq 1 (and with $N \geq 2$), two partially populated polaritonic states that were otherwise wrongfully ordered become disentangled, yielding one populated bright state and one unpopulated dark state.

RESULTS

Two parameters are varied in the simulations: the number of atoms N from 0 to 30, and the cavity vacuum field strength $\mathcal{E}_c$ from 0 to 5.14 GV/m. The excited-state population $P(N, \mathcal{E}_c)$, 503 fs after initial excitation, is evaluated and serves as a measure for the influence of the cavity coupling on the dissociation reaction. This remaining population is the portion of the wave function that has not been absorbed in the dissociative limit of the potential energy surfaces. Thus, P measures the stabilization of the molecule with respect to field-free case ($\mathcal{E}_c = 0$) where excited MgH^+ molecule fully dissociates via state $|C\rangle$. The population $P(N, \mathcal{E}_c)$ is shown in Figure 2 (detailed visualizations of selected time evolutions of the populations are available in the Supporting Information).

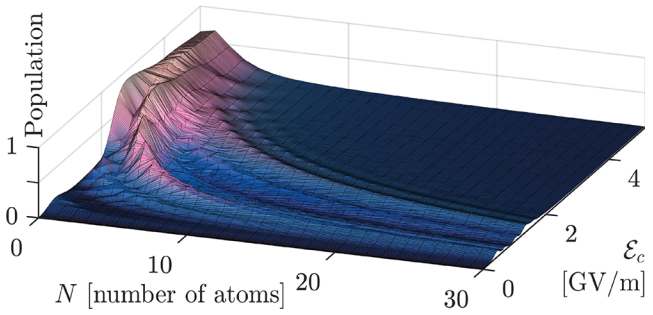

Figure 2. "Population" here describes a fraction of stable undissociated molecules and varies with the number of atoms in the ensemble N and with cavity vacuum field strength $\mathcal{E}_c$. A population of 0 means molecules have fully dissociated into Mg and H^+.

Several observations emerge: for a single molecule ($N = 0$) a sudden jump in population is observed, and for an increasing number of atoms the population is overall decreasing. The population is following a repeating pattern as $\mathcal{E}_c$ is increased for constant N (excluding smaller atomic ensembles, $N \gtrsim 2$): two larger local maxima are observed with smaller local maxima in-between. For larger values of $\mathcal{E}_c$ the molecule almost fully dissociates ($P(N, \mathcal{E}_c) \to 0$). The position of the two major maxima varies slowly with N creating two ridges in Figure 2.

For a qualitative understanding of the dynamics that generate the observed population, potential energy surfaces in the polariton basis are shown for selected values of N and $\mathcal{E}_c$ in Figures 3 and 4. Figure 3 shows how the polaritonic states are affected by introducing atoms into the cavity. With no atoms ($N = 0$), a vertical molecular excitation brings the system into the upper polariton state (yellow curve, Figure 3a), which has $|C, 0\rangle$ character in the Franck–Condon region. The

https://dx.doi.org/10.1021/acs.jpca.0c03867
J. Phys. Chem. A 2020, 124, 4672−4677

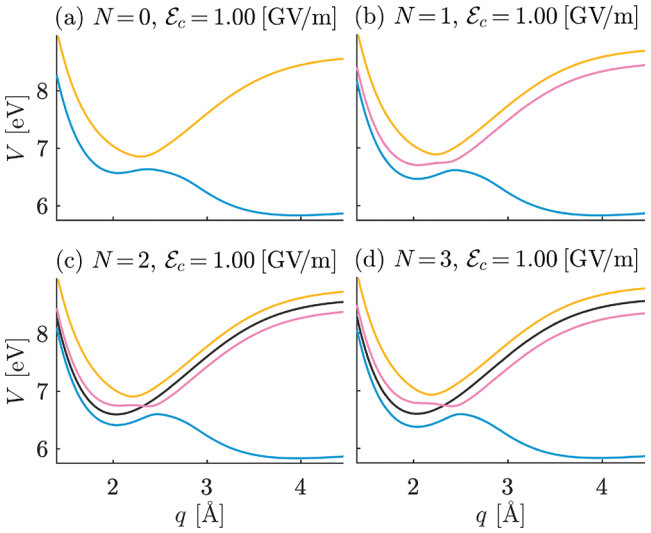

Figure 3. Potential energy curves in the polariton basis for an increasing number of atoms and a constant field strength, $\mathcal{E}_c$ = 1.00 GV/m. (a) The blue and the yellow curves are the lower and upper polariton states, respectively. (b) An ensemble with a single atom (N = 1) creates a middle polariton state (pink curve), which couples to the upper and lower polariton state. (c, d) Adding further atoms to the ensemble introduces degenerate states that are decoupled from all other (dark states, black curves).

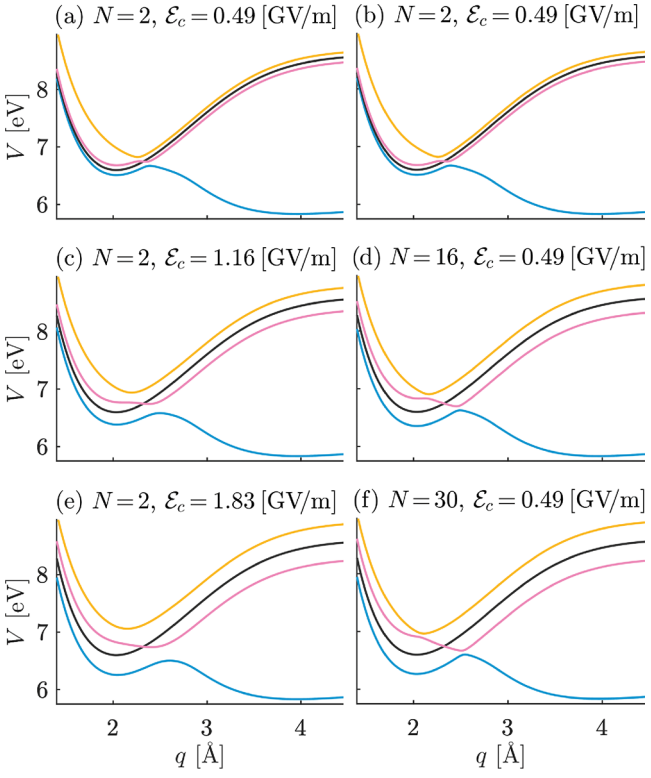

Figure 4. Potential energy curves in the polariton basis for an increasing number of atoms compared to increasing field strength. The left column (a, c, e) shows the effect of increasing field strength on the polariton states. The right column (b, d, f), shows the effect of an increasing number of atoms on the polariton states.

addition of a single atom creates a middle polariton state (pink curve, Figure 3b) that is coupled to the upper and lower polariton states. Here, a vertical molecular excitation still can populate the upper polariton state, but only for small collective Rabi splittings (i.e., small N and $\mathcal{E}_c$). For large Rabi splittings (i.e., large N or $\mathcal{E}_c$), the system is instead excited into the middle polariton state. The addition of further atoms (N > 2) introduces more degenerate dark states (black curve, Figure 3c,d) that are decoupled from the three active polariton states (lower, middle, and upper). For an arbitrary number of N atoms, there are $N-1$ dark states, which all have the character of an atomic excitation for all q.[28] Because there are only three active polariton states, all analysis and interpretations of the results can be done in terms of these three states alone, for any number of atoms N > 0.

Figure 4 shows a comparison of the effects of an increasing number of atoms N versus an increasing vacuum field strength $\mathcal{E}_c$. A crucial difference between increasing $\mathcal{E}_c$ (Figure 4a,c,e), and increasing N (Figure 4b,d,f) is the effect on the avoided crossings. The vacuum field strength $\mathcal{E}_c$ affects the splitting at the avoided crossings between the upper and middle polariton states as well as the middle and lower polariton states and for all nuclear distances q. This splitting for each avoided crossing is approximately the Rabi single-molecule splitting ($2\mathcal{E}_c\mu_m$). Increasing N causes a splitting between the upper and lower polariton states, which is approximately equal to the collective Rabi splitting ($2\sqrt{N}\mathcal{E}_c\mu_m$), but the energy gap at the two avoided crossings remains approximately equal to the single-molecule Rabi splitting ($2\mathcal{E}_c\mu_m$) for N = 0. For both increasing N and $\mathcal{E}_c$ a growing spatial separation along q is observed between the two avoided crossings.[3]

DISCUSSION

The formation of dark states and active (bright) states in this model can be understood in relation to the Dicke model.[40] In a pure Dicke model, where there are only atoms, the upper and lower polariton states can be populated by optical excitations, but all other excited states are uncoupled and thus considered dark states. Replacing one atom with a molecule turns a previously dark state (between upper and lower polariton states) active.[28] We name this active state a middle polariton state, and it is shown as the pink curve in Figure 3. It appears since the added nuclear degree of freedom tunes the molecule out of resonance with the atoms, for all q except at the curve crossing point. This finding is consistent with earlier work where an ensemble consisting of only molecules yields only bright states and no decoupled dark states.[27]

From Figure 2 it is clear that the number of atoms, N, and the field strength, $\mathcal{E}_c$, influence the dissociation of the MgH^+ molecule differently. The case of N = 0 corresponds to the molecular JC model. Here the Rabi splitting between polariton states is directly determined by $\mu_m\varepsilon_c$,[16,17] and increased stability for larger values of $\mathcal{E}_c$ can be understood as a separation of the upper polariton state from the lower polariton state (see Figure 3a). Increasing N, for a fixed value of $\mathcal{E}_c$, does however not have the same effect. The typical Rabi splitting for the different values of q behaves like a collective Rabi splitting ($\sim\sqrt{N}\mu_m\mathcal{E}_c$), while the splitting, particularly at the avoided crossings, behave like the single-molecule Rabi splitting ($\sim\mu_M\mathcal{E}_c$); see for example Figure 4f. The middle polariton state thus provides an efficient channel for dissociation, and the stability that a single molecule

https://dx.doi.org/10.1021/acs.jpca.0c03867
J. Phys. Chem. A 2020, 124, 4672−4677

experiences disappears as atoms are added to the cavity, even in the case of strong cavity coupling (large $\mathcal{E}_c$).

The large-scale structure in Figure 2 shows two ridges that appear when $N \gtrsim 2$. Inspection of the wave packet dynamics reveals that these structures are caused by two different effects. The first effect is a beneficial interplay between constructive and destructive interference at the avoided crossings, which prevents the wave packet from populating dissociation channels.[41] The first ridge with respect to an increase in $\mathcal{E}_c$ is caused by such beneficial interference (at the avoided crossing between upper and middle polariton state). The second effect is the aforementioned decoupling of the upper polariton state due to increasing single-molecule Rabi splitting. The second ridge is caused by such isolation of polariton states. The region between these two maxima is due to the interplay of both effects. Here, the efficiency of the constructive and destructive interference is the main cause of rapid fluctuations in stability.

Even though the molecular stability generally decreases for increasing atoms numbers, it is still possible to increase stability by adding atoms. For $N \lesssim 10$ the increased molecular stability can be shifted significantly toward lower $\mathcal{E}_c$ at the cost of reduced peak stability. For larger N the increase in stability is significantly reduced but is still being shifted to even lower $\mathcal{E}_c$. For $N \gtrsim 10$ and $\mathcal{E}_c \gtrsim 2\ \mathrm{GV\,m^{-1}}$ the molecule always dissociates, and the reaction cannot be controlled effectively anymore. In this parameter regime, the middle polariton has predominantly molecular character and dictates the dynamics. Here the avoided crossings are spatially well separated along q, and the state characters of the upper and middle polariton state are swapped. The upper and lower polariton states are mainly of atomic/photonic character. An optical excitation now goes directly into the middle polariton state.

CONCLUSION

We have shown that the reactivity of an MgH^+ molecule is modified by collective strong coupling with Mg atoms. The model gives a clear mechanistic insight into the role of the middle polariton state, which emerges as a consequence of the nuclear degree of freedom. The calculations also show that collective Rabi splitting, as it is expected from the TC model, becomes a quantity that is an effective splitting but does not determine the dynamics. An increase in ensemble size (i.e., an increase in collective coupling strength) can thus not be used as a substitute for single-molecule coupling strength. More strikingly, the ability to increase molecular stability by means of large single-molecule coupling disappears when the number of atoms is increased. This demonstrates that collective strong coupling cannot be explained in terms of the JC model even for a simple model system of one molecule and N two-level systems. The dissociation dynamics in the examined model is governed by two rather than one cavity-induced avoided crossings, and their positions depend on the number of atoms in the ensemble. The calculations also show that there is an interplay of several effects that allow using atoms to achieve a useful modification of the reactivities at lower vacuum field strengths.

ASSOCIATED CONTENT

Supporting Information

The Supporting Information is available free of charge at https://pubs.acs.org/doi/10.1021/acs.jpca.0c03867.

Detailed curves of Figure 2 one for each $N \in \{0, ..., 11\}$, molecular stability after excitation with classical pump pulse, molecular stability with constant transition dipole moment, molecular stability after shorter 50 fs time evolution (PDF)

AUTHOR INFORMATION

Corresponding Authors

Eric Davidsson − *Department of Physics, Stockholm University, Albanova University Centre, SE-106 91 Stockholm, Sweden;* orcid.org/0000-0003-1030-0640; Email: eric.davidsson@fysik.su.se

Markus Kowalewski − *Department of Physics, Stockholm University, Albanova University Centre, SE-106 91 Stockholm, Sweden;* orcid.org/0000-0002-2288-2548; Email: markus.kowalewski@fysik.su.se

Complete contact information is available at: https://pubs.acs.org/10.1021/acs.jpca.0c03867

Notes

The authors declare no competing financial interest.

ACKNOWLEDGMENTS

The authors thank Ágnes Vibók and Gábor Halász for fruitful discussions. Support from the Swedish Research Council (Grant VR 2018-05346) is acknowledged. This project has received funding from the European Research Council (ERC) under the European Union's Horizon 2020 research and innovation program (Grant Agreement No. 852286).

REFERENCES

(1) Hertzog, M.; Wang, M.; Mony, J.; Börjesson, K. Strong Light-Matter Interactions: A New Direction Within Chemistry. *Chem. Soc. Rev.* **2019**, *48*, 937−961.

(2) Herrera, F.; Spano, F. C. Cavity-Controlled Chemistry in Molecular Ensembles. *Phys. Rev. Lett.* **2016**, *116*, 238301.

(3) Feist, J.; Galego, J.; Garcia-Vidal, F. J. Polaritonic Chemistry with Organic Molecules. *ACS Photonics* **2018**, *5*, 205−216.

(4) Ribeiro, R. F.; Martínez-Martínez, L. A.; Du, M.; Campos-Gonzalez-Angulo, J.; Yuen-Zhou, J. Polariton Chemistry: Controlling Molecular Dynamics with Optical Cavities. *Chem. Sci.* **2018**, *9*, 6325−6339.

(5) Stranius, K.; Hertzog, M.; Börjesson, K. Selective Manipulation of Electronically Excited States through Strong Light-Matter Interactions. *Nat. Commun.* **2018**, *9*, 2273.

(6) Herrera, F.; Spano, F. C. Theory of Nanoscale Organic Cavities: The Essential Role of Vibration-Photon Dressed States. *ACS Photonics* **2018**, *5*, 65−79.

(7) Munkhbat, B.; Wersäll, M.; Baranov, D. G.; Antosiewicz, T. J.; Shegai, T. Suppression of Photo-Oxidation of Organic Chromophores by Strong Coupling to Plasmonic Nanoantennas. *Sci. Adv.* **2018**, *4*, eaas9552.

(8) Csehi, A.; Vibók, A.; Halász, G. J.; Kowalewski, M. Quantum Control with Quantum Light of Molecular Nonadiabaticity. *Phys. Rev. A: At., Mol., Opt. Phys.* **2019**, *100*, 053421.

(9) Xiang, B.; Ribeiro, R. F.; Dunkelberger, A. D.; Wang, J.; Li, Y.; Simpkins, B. S.; Owrutsky, J. C.; Yuen-Zhou, J.; Xiong, W. Two-Dimensional Infrared Spectroscopy of Vibrational Polaritons. *Proc. Natl. Acad. Sci. U. S. A.* **2018**, *115*, 4845−4850.

(10) Simpkins, B. S.; Fears, K. P.; Dressick, W. J.; Spann, B. T.; Dunkelberger, A. D.; Owrutsky, J. C. Spanning Strong to Weak Normal Mode Coupling between Vibrational and Fabry−Pérot Cavity Modes through Tuning of Vibrational Absorption Strength. *ACS Photonics* **2015**, *2*, 1460−1467.

(11) Bisht, A.; Cuadra, J.; Wersäll, M.; Canales, A.; Antosiewicz, T. J.; Shegai, T. Collective Strong Light-Matter Coupling in Hierarchical Microcavity-Plasmon-Exciton Systems. *Nano Lett.* **2019**, *19*, 189−196.
(12) Hutchison, J. A.; Schwartz, T.; Genet, C.; Devaux, E.; Ebbesen, T. W. Modifying Chemical Landscapes by Coupling to Vacuum Fields. *Angew. Chem., Int. Ed.* **2012**, *51*, 1592−1596.
(13) Schwartz, T.; Hutchison, J. A.; Léonard, J.; Genet, C.; Haacke, S.; Ebbesen, T. W. Polariton Dynamics under Strong Light−Molecule Coupling. *ChemPhysChem* **2013**, *14*, 125−131.
(14) Zhong, X.; Chervy, T.; Wang, S.; George, J.; Thomas, A.; Hutchison, J. A.; Devaux, E.; Genet, C.; Ebbesen, T. W. Non-Radiative Energy Transfer Mediated by Hybrid Light-Matter States. *Angew. Chem., Int. Ed.* **2016**, *55*, 6202−6206.
(15) Jaynes, E. T.; Cummings, F. W. Comparison of Quantum and Semiclassical Radiation Theories with Application to the Beam Maser. *Proc. IEEE* **1963**, *51*, 89−109.
(16) Kowalewski, M.; Bennett, K.; Mukamel, S. Non-Adiabatic Dynamics of Molecules in Optical Cavities. *J. Chem. Phys.* **2016**, *144*, 054309.
(17) Galego, J.; Garcia-Vidal, F. J.; Feist, J. Cavity-Induced Modifications of Molecular Structure in the Strong-Coupling Regime. *Phys. Rev. X* **2015**, *5*, 041022.
(18) Flick, J.; Ruggenthaler, M.; Appel, H.; Rubio, A. Atoms and Molecules in Cavities, from Weak to Strong Coupling in Quantum-Electrodynamics (QED) Chemistry. *Proc. Natl. Acad. Sci. U. S. A.* **2017**, *114*, 3026−3034.
(19) Csehi, A.; Kowalewski, M.; Halász, G. J.; Vibók, Á. Ultrafast Dynamics in the Vicinity of Quantum Light-Induced Conical Intersections. *New J. Phys.* **2019**, *21*, 093040.
(20) Kowalewski, M.; Bennett, K.; Mukamel, S. Cavity Femtochemistry: Manipulating Nonadiabatic Dynamics at Avoided Crossings. *J. Phys. Chem. Lett.* **2016**, *7*, 2050−2054.
(21) Vendrell, O. Coherent Dynamics in Cavity Femtochemistry: Application of the Multi-Configuration Time-Dependent Hartree Method. *Chem. Phys.* **2018**, *509*, 55−65.
(22) Groenhof, G.; Climent, C.; Feist, J.; Morozov, D.; Toppari, J. J. Tracking Polariton Relaxation with Multiscale Molecular Dynamics Simulations. *J. Phys. Chem. Lett.* **2019**, *10*, 5476−5483.
(23) Ojambati, O. S.; Chikkaraddy, R.; Deacon, W. D.; Horton, M.; Kos, D.; Turek, V. A.; Keyser, U. F.; Baumberg, J. J. Quantum Electrodynamics at Room Temperature Coupling a Single Vibrating Molecule with a Plasmonic Nanocavity. *Nat. Commun.* **2019**, *10*, 1−7.
(24) Peters, V. N.; Faruk, M. O.; Asane, J.; Alexander, R.; Peters, D. A.; Prayakarao, S.; Rout, S.; Noginov, M. A. Effect of Strong Coupling on Photodegradation of the Semiconducting Polymer P3HT. *Optica* **2019**, *6*, 318−325.
(25) Tavis, M.; Cummings, F. W. The Exact Solution of N Two Level Systems Interacting with a Single Mode, Quantized Radiation Field. *Phys. Lett. A* **1967**, *25*, 714−715.
(26) Dicke, R. H. Coherence in Spontaneous Radiation Processes. *Phys. Rev.* **1954**, *93*, 99−110.
(27) Ulusoy, I. S.; Gomez, J. A.; Vendrell, O. Modifying the Nonradiative Decay Dynamics through Conical Intersections via Collective Coupling to a Cavity Mode. *J. Phys. Chem. A* **2019**, *123*, 8832−8844.
(28) Szidarovszky, T.; Halász, G. J.; Vibók, Á. *Mix It Up: Striking Nonadiabatic Fingerprint in an Entangled Atom-Molecule-Photon Polariton*. arXiv e-prints 2019, arXiv:1912.03916.
(29) Flick, J.; Appel, H.; Ruggenthaler, M.; Rubio, A. Cavity Born-Oppenheimer Approximation for Correlated Electron-Nuclear-Photon Systems. *J. Chem. Theory Comput.* **2017**, *13*, 1616−1625.
(30) Galego, J.; Garcia-Vidal, F. J.; Feist, J. Cavity-Induced Modifications of Molecular Structure in the Strong-Coupling Regime. *Phys. Rev. X* **2015**, *5*, 041022.
(31) Kowalewski, M.; Bennett, K.; Mukamel, S. Cavity Femtochemistry: Manipulating Nonadiabatic Dynamics at Avoided Crossings. *J. Phys. Chem. Lett.* **2016**, *7*, 2050−2054.
(32) Kowalewski, M. Quantendynamik Isolierter Molekularer Systeme. Ph.D. Thesis, Ludwig-Maximilians-Universität:München, 2012.
(33) Kahra, S.; Leschhorn, G.; Kowalewski, M.; Schiffrin, A.; Bothschafter, E.; Fuß, W.; de Vivie-Riedle, R.; Ernstorfer, R.; Krausz, F.; Kienberger, R.; et al. Controlled Delivery of Single Molecules into Ultra-Short Laser Pulses, a Molecular Conveyor Belt. *Nat. Phys.* **2012**, *8*, 238−242.
(34) Werner, H. J.; Knowles, P. J.; Lindh, R.; Manby, F. R.; Schütz, M.; et al. *MOLPRO, Version 2006.1, a Package of Ab Initio Programs*, 2006.
(35) Widmark, P.-O.; Malmqvist, P.-Å.; Roos, B. O. Density Matrix Averaged Atomic Natural Orbital (ANO) Basis Sets for Correlated Molecular Wave Functions. *Theoretica chimica acta* **1990**, *77*, 291−306.
(36) Widmark, P.-O.; Persson, B. J.; Roos, B. O. Density Matrix Averaged Atomic Natural Orbital (ANO) Basis Sets for Correlated Molecular Wave Functions. *Theoretica Chimica Acta* **1991**, *79*, 419−432.
(37) Kramida, A.; Ralchenko, Yu.; Reader, J.; NIST ASD Team. NIST Atomic Spectra Database Lines Data. In *NIST Atomic Spectra Database (ver. 5.7.1)*; available: https://physics.nist.gov/asd; National Institute of Standards and Technology: Gaithersburg, MD, 2019 (retrieved November 28, 2019); https://bit.ly/2qXjmgP.
(38) Nissen, A.; Karlsson, H. O.; Kreiss, G. A Perfectly Matched Layer Applied to a Reactive Scattering Problem. *J. Chem. Phys.* **2010**, *133*, 054306.
(39) Tal-Ezer, H.; Kosloff, R. An Accurate and Efficient Scheme for Propagating the Time Dependent Schrödinger Equation. *J. Chem. Phys.* **1984**, *81*, 3967−3971.
(40) Garraway, B. M. The Dicke Model in Quantum Optics: Dicke Model Revisited. *Philos. Trans. R. Soc., A* **2011**, *369*, 1137−1155.
(41) Wang, D.; Åsa, L.; Karlsson, H. O.; Hansson, T. Molecular Quantum Wavepacket Revivals in Coupled Electronic States. *Chem. Phys. Lett.* **2007**, *449*, 266−271.

https://dx.doi.org/10.1021/acs.jpca.0c03867
J. Phys. Chem. A 2020, 124, 4672−4677